

## Supporting Information

### **Bioanalytical method for NAD<sup>+</sup> detection in blood plasma utilizing solution-phase *Candida boidinii* formate dehydrogenase and electrochemical detection**

Wichit Taron,<sup>a</sup> Tharinda Kasemphong,<sup>b</sup> Pachanuporn Sunon,<sup>a</sup> Keerakit Kaewket,<sup>a</sup> Nuntaporn Kamonsutthipaijit,<sup>c</sup> James R. Ketudat-Cairns,<sup>b</sup> Gun Bhakdisongkhrum,<sup>d</sup> Warut Tulalamba,<sup>e,f</sup> Supakmongkon Sanguansuk,<sup>g</sup> Vip Viprakasit,<sup>e,h</sup> Kamonwad Ngamchuea<sup>b\*</sup>

<sup>a</sup> Institute of Research and Development, Suranaree University of Technology, 111 University Avenue, Muang District, Nakhon Ratchasima 30000, Thailand

<sup>b</sup> School of Chemistry, Institute of Science, Suranaree University of Technology, 111 University Avenue, Muang District, Nakhon Ratchasima 30000, Thailand

<sup>c</sup> Synchrotron Light Research Institute, 111 University Avenue, Suranaree, Muang District, Nakhon Ratchasima 30000, Thailand

<sup>d</sup> School of Medicine, Institute of Medicine, Suranaree University of Technology, 111 University Avenue, Muang District, Nakhon Ratchasima 30000, Thailand

<sup>e</sup> Siriraj Thalassemia Center, Faculty of Medicine Siriraj Hospital, Mahidol University, Bangkok, Thailand

<sup>f</sup> Research Division, Faculty of Medicine Siriraj Hospital, Mahidol University, Bangkok, Thailand

<sup>g</sup> Research & Development Laboratory, ATGenes Limited Company, Bangkok, Thailand

<sup>h</sup> Department of Pediatrics, Faculty of Medicine Siriraj Hospital, Mahidol University, Bangkok, Thailand

\*Corresponding author: Kamonwad Ngamchuea, School of Chemistry, Institute of Science, Suranaree University of Technology, 111 University Avenue, Muang District, Nakhon Ratchasima 30000, Thailand. Email: kamonwad@g.sut.ac.th. Tel: +66 (0) 44 224 637

## S1 UV-visible spectra of CbFDH enzymatic reactions

As discussed in the main text, UV-visible spectrophotometry (200–400 nm) was used to monitor enzymatic reactions involving CbFDH, formate, and  $\text{NAD}^+$ , verifying the formation of NADH. The corresponding spectra are shown in Figure S1 below, with a detailed discussion provided in the main text.

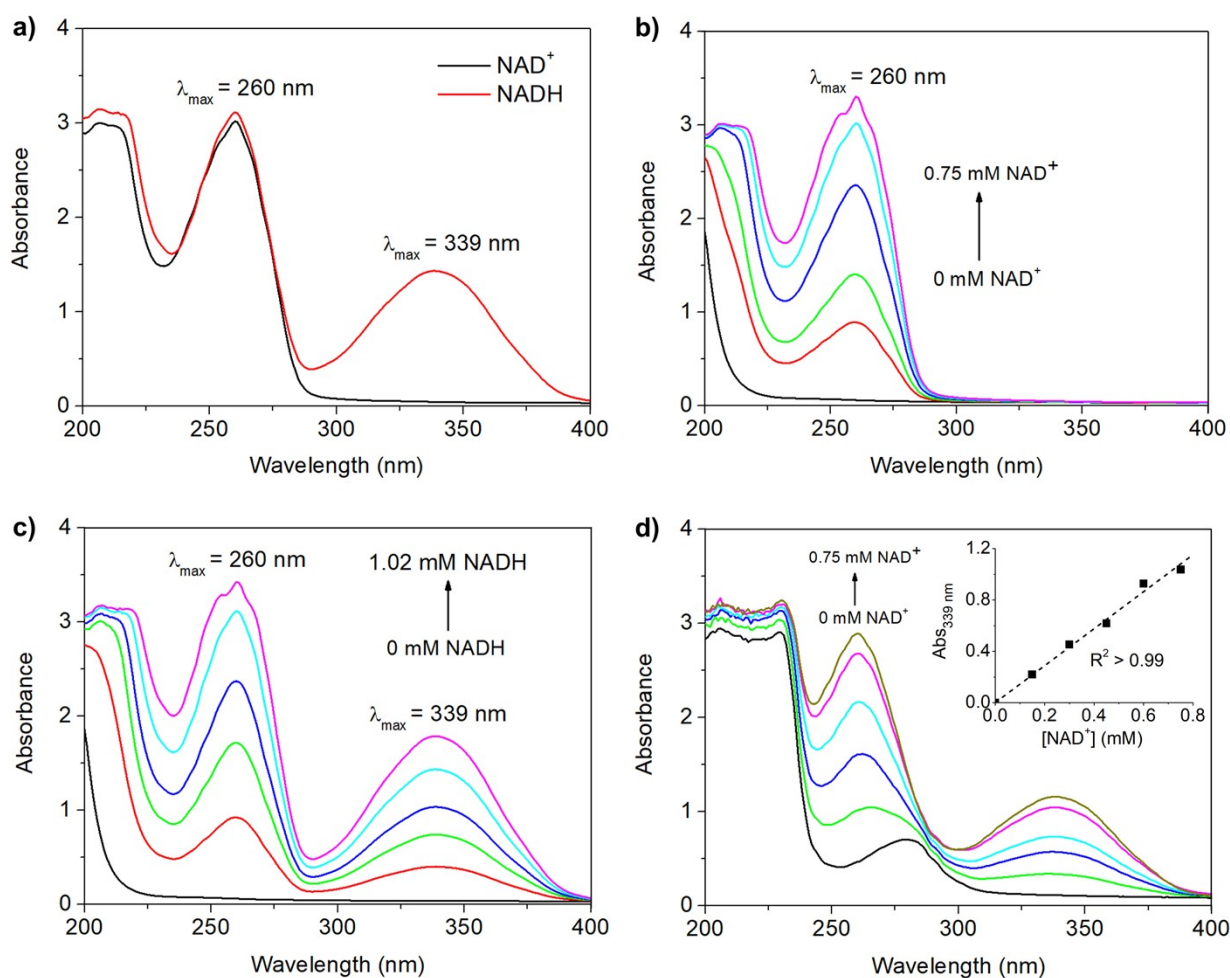


**Figure S1:** UV-vis spectra of **a)** 0.6 mM  $\text{NAD}^+$  vs. 0.8 mM NADH; **b)** varying concentrations of  $\text{NAD}^+$  (0, 0.15, 0.30, 0.45, 0.60, and 0.75 mM); **c)** varying concentrations of NADH (0, 0.20, 0.40, 0.60, 0.80, and 1.02 mM); **d)** a mixture of 320 mM formate,  $3 \text{ U mL}^{-1}$  CbFDH, and varying concentrations of  $\text{NAD}^+$  (0, 0.15, 0.30, 0.45, 0.60, and 0.75 mM) in 100-fold diluted blood plasma.

## S2 Analytical performance for non-enzymatic detection

Figures 2b and 2c in the main text display cyclic voltammograms of  $\text{NAD}^+$  and NADH, respectively, over various concentrations under non-enzymatic conditions at a scan rate of  $25 \text{ mV s}^{-1}$ . For  $\text{NAD}^+$ , the electrochemical response exhibits a linear range from  $0.43 \text{ }\mu\text{M}$  to  $10 \text{ mM}$ , with a sensitivity of  $7.10 \pm 0.17 \text{ }\mu\text{A mM}^{-1}$ , a limit of detection ( $3s_b/m$ ) of  $0.13 \text{ }\mu\text{M}$ , and a limit of quantification ( $10s_b/m$ ) of  $0.43 \text{ }\mu\text{M}$ . Meanwhile, NADH shows an oxidation response with a linear range of  $0.57 \text{ }\mu\text{M}$  to  $12 \text{ mM}$ , achieving a sensitivity of  $9.98 \pm 0.10 \text{ }\mu\text{A mM}^{-1}$ , a limit of detection ( $3s_b/m$ ) of  $0.17 \text{ }\mu\text{M}$ , and a limit of quantification ( $10s_b/m$ ) of  $0.57 \text{ }\mu\text{M}$ .

### S3 Tafel analysis

To assess the electron transfer kinetics, Tafel analysis was performed according to equation 2 in the main text. The plot of  $\ln I$  vs.  $E$  (Figure S2) was constructed using current values within 15–50% of the peak current in order to minimize the influence of mass transport.<sup>35</sup> The slope of this plot yielded a value of  $\frac{n' + \beta_{n+1}'}{n+1}$  of  $0.53 \pm 0.01$ , indicating that the initial electron transfer is the rate-determining step. The corresponding apparent anodic transfer coefficient  $\beta_{n+1}'$  for this step was therefore  $0.53 \pm 0.01$ , as discussed in the main text.

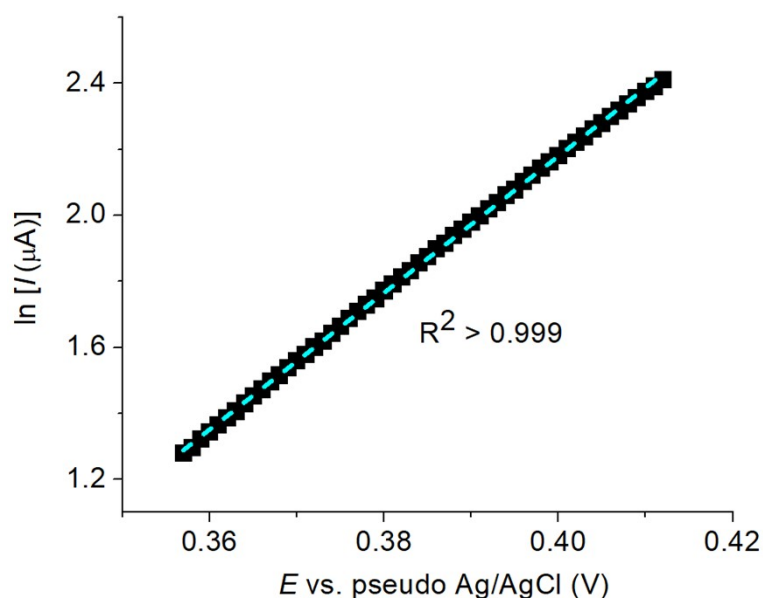


**Figure S2:** The plot of  $\ln I$  vs.  $E$  in the Tafel analysis of 5 mM NADH in 0.1 M PBS pH 7.6 and 0.1 M KCl at a scan rate of  $10 \text{ mV s}^{-1}$ . Current values used in the analysis were taken within 15–50% of the peak current.

#### S4 Scan rate studies: $\log I_p$ versus $\log v$ plot

The plot of  $\log I_p$  vs.  $\log v$  (Figure S3) exhibited a slope of 0.46 ( $R^2 > 0.999$ ), which closely approximates the theoretical value of 0.5. This agreement supports the conclusion that the NADH oxidation at graphite SPEs is predominantly diffusion-controlled, as discussed in the main text.

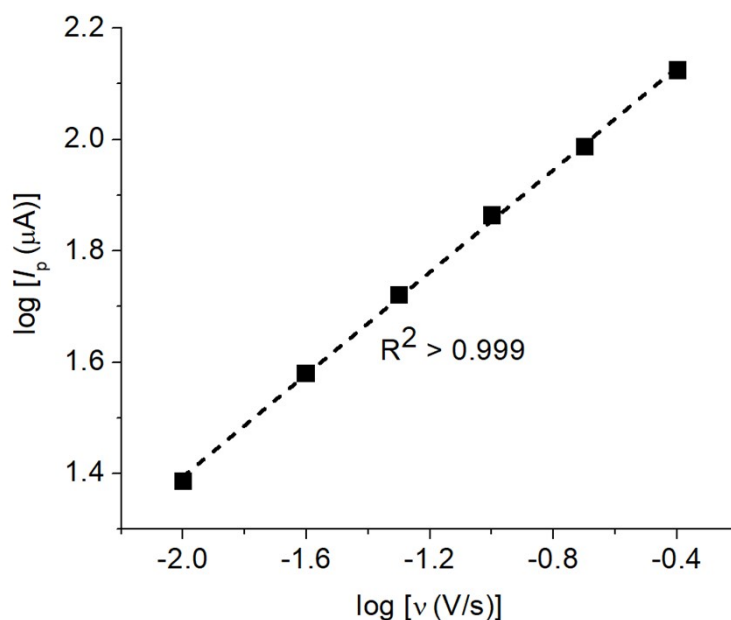


**Figure S3:**  $\log I_p$  vs.  $\log v$  plot of 5 mM NADH in 0.1 M PBS pH 7.6 and 0.1 M KCl, at scan rates ranging from 10 to 400  $\text{mV s}^{-1}$ .